CONF-851217--21

THE HARDNESS OF ION IMPLANTED CERAMICS*

W. C. OLIVER,** C. J. McHARGUE,** G. C. FARLOW,*** AND C. W. WHITE**
**Oak Ridge National Laboratory, Oak Ridge, Tennessee 37831
***Wright State University, Dayton, Ohio

CONF-851217--21

DE86 004771

ABSTRACT

It has been established that the wear behavior of ceramic materials can be modified through ion implantation. Studies have been done to characterize the effect of implantation on the structure and composition of ceramic surfaces. To understand how these changes affect the wear properties of the ceramic, other mechanical properties must be measured. To accomplish this, a commercially available ultra low load hardness tester has been used to characterize Al_2O_3 with different implanted species and doses. The hardness of the base material is compared with the highly damaged crystalline state as well as the amorphous material.

INTRODUCTION

The mechanical properties of most ceramics are extremely flaw dependent. The surface preparation of such materials often determine the number and size distribution of the flaws and therefore the strength of the sample. This is demonstrated by the variety of strengths reported for single crystal Al_2O_3. These values range from 525 MPa for ground surfaces to 1.59 GPa for gas polished material [1,2].

This characteristic of ceramics makes them obvious candidates for special surface treatment processes such as ion implantation. Considerable work has been done to characterize ion implanted ceramics. Several reviews of the literature are now available [3,4]. Rutherford backscattering (RBS) has been used to probe the chemical and structural changes caused by implantation with a variety of ions and conditions in a variety of substrates [5,6]. It has been documented that amorphous layers can be achieved if the lattice damage exceeds a critical level in some ceramics [6,7]. These results have been confirmed by examining cross sectional specimens of the surfaces in the transmission electron microscope (TEM).

Characterizing the surfaces of ion implanted ceramics mechanically is more difficult. Low load (10 g or greater) Vickers and Knoop indentation tests have been used on a variety of ion substrate systems [1,5-8]. Although in some cases the depth of such indents approaches the implanted depth, the radius of the plastic zone of such an indent is many times the depth. In addition, the dimensions of such indents are so small that, even with excellent optical systems, they are very difficult to measure. The results of such tests are interesting and may indicate trends but are at best qualitative. Scratch tests have also been used to show beneficial effects from ion implantation of ceramics [9,10]. Finally, bend tests of specimens with ion implanted surfaces have shown distinct strength improvements. This is the most convincing mechanical data in favor of such treatments [1].

A special ultra low load hardness tester has been used successfully to characterize the mechanical properties of ion implanted metals [11]. This

---

*Research sponsored by the Division of Materials Sciences, U.S. Department of Energy, under contract W-7405-eng-26 with the Martin Marietta Energy Systems, Inc.

paper reports the initial studies of ion implanted ceramics with such a system. Three implanted conditions of Al_2O_3 will be discussed, two in which the surface is damaged, but remains crystalline, and a third in which the surface region is amorphous.

EXPERIMENTAL

Ion Implantation and Rutherford Backscattering

Three implantation conditions were used to implant c-axis oriented sapphire single crystal specimens. The sapphire had been mechanically polished to a 1-μin. finish. The specimens were then annealed in air for five days at 1400°C to remove any mechanical damage. The implantation conditions and the ranges, straggling, peak concentrations, and the position and level of the peak damage are shown in Table I. These specimens were prepared in a system with a vacuum of 10^{-6} to 10^{-7} torr.

Table I. RBS Results for Ion Implanted Al_2O_3*

Implantation conditions	Range R_p (nm)	ΔR_p (nm)	Cr:Al ratio peak	dpa (peak)	Depth of peak damage (nm)	Crystalline or amorphous
4×10^{16} Cr/cm^2 150 keV 300 K	138	49	0.03	12.7	31	C
1×10^{17} Cr/cm^2 280 keV 300 K	160	73	0.09	109	86	C
4×10^{16} Al/cm^2 90 keV* 4×10^{16} O/cm^2 55 keV 77 K	80** 80**					A (to depth of 155 nm)

*2 MeV ^{4}He.
**Calculated.

The microindentation experiments were carried out on a Nanoindenter (Nano Instruments, Inc.). The system is shown schematically in Fig. 1. the resolution of the displacement sensing system is 0.16 nm. The loading systems resolution is 0.4 μN. By knowing the depth of the indent, the load and the functional relationship between the depth and the contact area, the hardness can be calculated. The entire system is automated so that multiple indents can be made in a single computer run. This feature of the system allows adequate statistical certainty in the results to be obtained in a reasonable length of time.

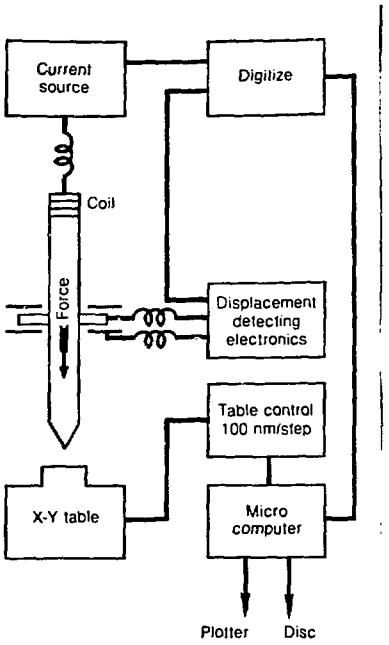

Fig. 1. Schematic of Nanoindenter.

The unimplanted results were obtained from portions of the specimens that were masked during implantation process. The implanted surfaces were then tested without reorienting the specimens, thus avoiding effects originating from the orientation of the indenter with respect to the sample crystallography.

RESULTS AND DISCUSSION

Structural

The RBS results for three of the implantation conditions are shown in Figs. 2–4. Figures 2 and 3 show that for the samples implanted with chromium at 150 and 280 keV, the implanted regions are damaged but remain crystalline. Figure 4 shows that the specimen implanted with aluminum and oxygen contains a surface amorphous layer extending from the surface to a depth of 155 nm. These results have been confirmed elsewhere using cross sections of the implanted regions studied with the TEM [7].

Mechanical Properties

The most direct way of learning about the effects of ion implantation on the mechanical properties of surfaces is to measure the differences between the implanted and unimplanted conditions. This is particularly true for hardness testing where indentation size effects in simple materials are not well understood. Hence, it is necessary to measure the properties of the substrate first. In this case, the substrate is sapphire with the c-axis perpendicular to the surface prepared as previously described.

The indentation results for the substrate material showed two distinct load-indenter displacement curves. The two curves are shown in Figs. 5(a) and (b). Of the ten indents made in this material, four were similar to and averaged into Fig. 5(a). Six of the curves were similar to and averaged into Fig. 5(b). Figure 5(a) is similar in shape to indents made in ductile materials (metals and plastics). However, the elastically recovered

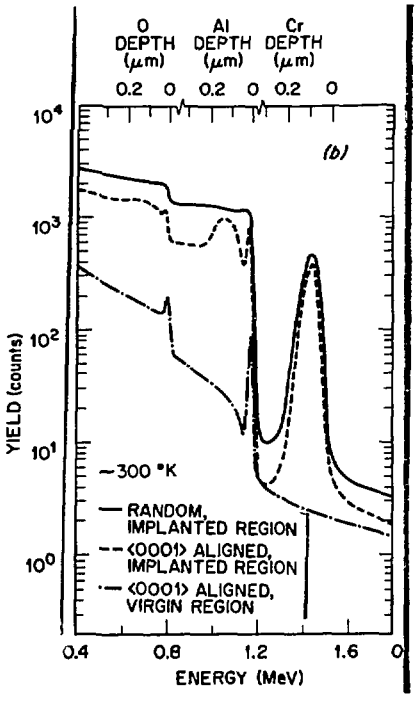

Fig. 2. Rutherford-backscattering result (2 MeV ^{4}He) for specimen implanted with 150 keV chromium.

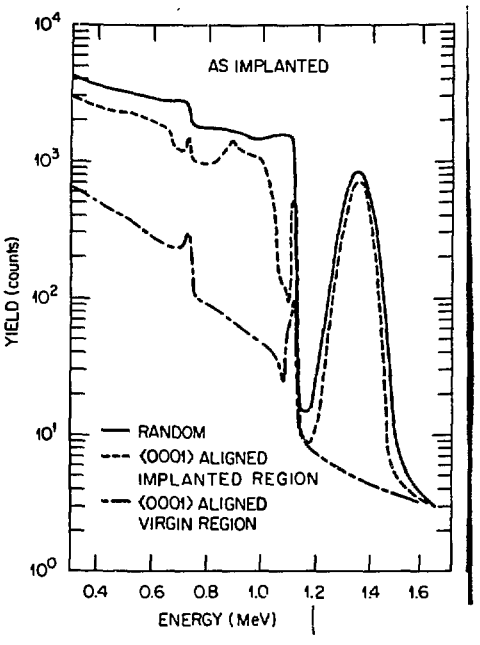

Fig. 3. Rutherford-backscattering result (2 MeV ^{4}He) for specimen implanted with 280 keV chromium.

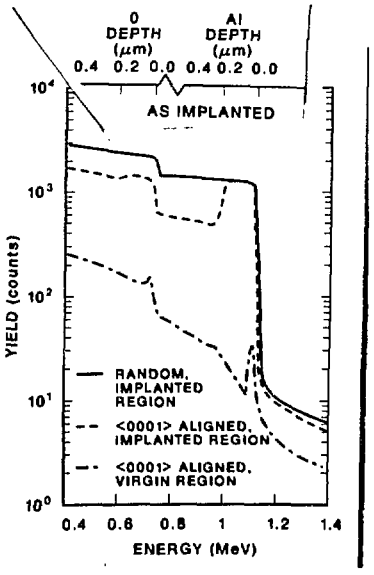

Fig. 4. Rutherford-backscattering result (1 MeV ^{4}He) for specimen implanted with 90 keV aluminum and 55 keV oxygen.

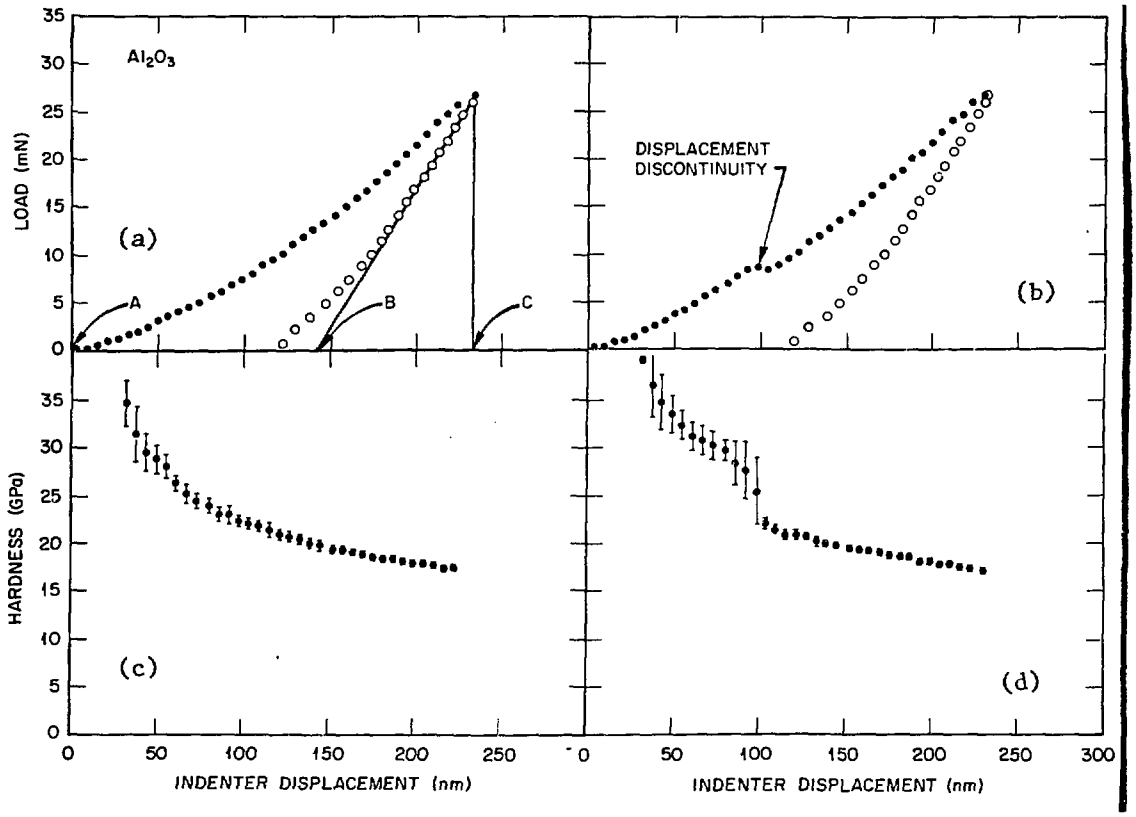

Fig. 5. Microindentation results for c-axis oriented sapphire, • loading, o unloading.

indenter displacement represented by the unloading portion of the curve is greater than in most metals. This is due to the higher hardness to modulus (H/E) ratio of sapphire as compared to most metals. Figure 5(b) shows the obvious initiation and propagation of some type of flaw near the indenter. The discontinuity of the displacement at a given load clearly indicates that the initiation of the flaw requires higher stresses than its propagation. Some possible flaws are cracks, twins, and dislocations. The curve shown in Figs. 5(a) and (b) are identical subsequent to the displacement discontinuity. This observation indicates that four of the curves behaved as if the flaw was present from the beginning of the test [Fig. 5(a)]. This observation confirms that there is a population of flaws in the surface of the sample and that the mechanical properties of the sapphire are very flaw dependent.

The unloading portion of the load-indenter displacement curves can be used to calculate the modulus of the sample using the solutions to the elastic problem of axisymetric rigid punches indenting a semi-infinite solid as suggested originally by Stilwell and Tabor [12] and then refined by Shorshorov et al. [13]. Referring to Fig. 5(a):

$$\left.\frac{dY}{dW}\right|_{W_{max}} = \frac{\pi}{2} \cdot \frac{1}{\sqrt{A}} \cdot \frac{1}{E_r}$$

where $E_r = \left[\frac{1 - \nu_1^2}{E_1} + \frac{1 - \nu_2^2}{E_2}\right]^{-1}$

Y = elastic indenter displacement,

W = load,

A = area of the contact,

ν_1, E_1 = Poisson's ratio and the elastic modulus of the sample, and

ν_2, E_2 = Poisson's ratio and the elastic modulus of the sample indenter.

This analysis of the data obtained from unimplanted sapphires yields an average modulus of 539 GPa. This compares reasonably well with the published value of 502 GPa for C_{33} in sapphire at room temperature [14].

The hardness of the sapphire in the presence of the flaw is shown in Fig. 5(c). The hardnesses shown were calculated from the load-indenter displacement data shown in Fig. 5(a). The hardness shows a definite indentation size effect (ISE) (the hardness is not constant as the depth changes). The values range from 35 GPa at an indenter displacement of 40 nm to 18 GPa at 225 nm. It should be noted that the depth of the plastic indent spanned by this data ranges from 24 to 140 nm. The plastically deformed volume of material is approximately hemispherical with a radius of 7 to 14 times the plastic indent depth. The significance of such indentation size effects is questionable since their magnitude are critically dependent on the depth-to-area function used for the particular indenter. The error bars on all of the hardness versus indenter-displacement curves shown are two standard deviations in length. The standard deviation is calculated by averaging all of the data points from all the indents in a given material between a given depth plus or minus 3 nm.

The large elastic recovery can be accounted for by taking the plastic depth of the indent at any indenter displacement to be the indenter displacement multiplied by the ratio of the lengths AB by AC as shown in Fig. 5(a). The justification for this correction has been made by several previous authors [13,15,16]. Two assumptions are made with this type of correction: (1) that the modulus is constant as a function of depth and (2) during the relaxation, the projected area of the indent remains constant. The first assumption is certainly reasonable for sapphire. The second has been shown to be approximately correct for a wide variety of materials. When these corrections are made, the general shape of the curve would be unchanged, but the values would range from 90 GPa at 40 nm to 45 GPa at 225 nm. These values more accurately represent the plastic hardness of sapphire at these depths.

Figure 5(d) shows the calculated hardness values for the data shown in Fig. 5(b). The values for the hardness subsequent to the initiative event are identical to those shown in Fig. 5(c) at the same depths. Prior to the initiation of the flaws, the hardness is higher and the scatter in the results increases. In this region, the strength is probably controlled by existing flaws that are propagated at stress lower than the initiation

stress for the flaw(s) that causes the major displacement discontinuity shown in Fig. 5(b). The variation of the population of such flaws near the indenter causes the increased scatter in the results.

The load displacement curves for the implanted specimens are shown in Figs. 6(a)(b)(c). Figure 6(c) corresponds to the sample implanted with aluminum and oxygen so that an amorphous surface layer was formed. The results of eight indents are averaged into Fig. 6(a); ten into Fig. 6(b); and twelve into Fig. 6(c). Clearly, there are no discontinuities in the indenter displacement for the implanted materials. There are several possible causes for the absence of such discontinuity.

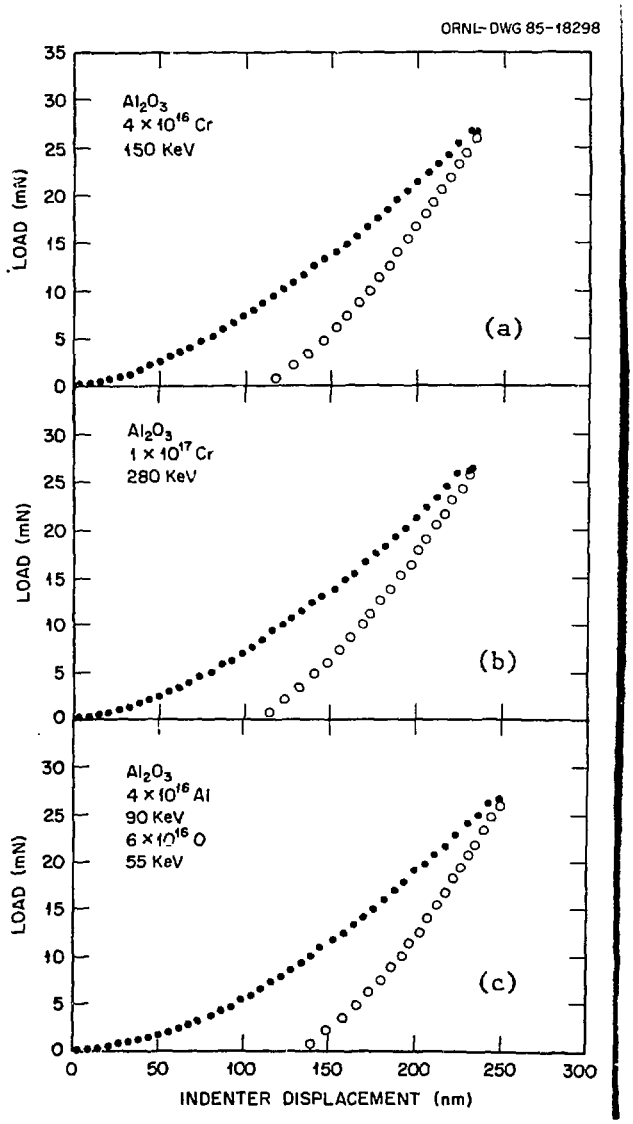

Fig. 6. Microindentation results for implanted sapphire, • loading, o unloading.

It is well known that implantation generates many defects in the surface of materials. Thus, the implantation may nucleate the flaws responsible for this effect. If that is the case, it would only be necessary to propagate these flaws. The other obvious possibility is that the implantation reduced the applied stress for nucleation to a very small value.

It is well established that implantation of metals can result in large residual stresses [17]. These stresses are often tensile in nature at the surface, compressive near the average range of the ions, and then finally tensile further into the material. Such surface tensile stresses would certainly increase the effective stresses associated with a given applied load and thus eliminate the displacement discontinuity shown in Fig. 5(a).

The modulus calculated from the sample with an amorphous sublayer [Fig. 6(c) yields a value of 479 GPa. This result is heavily influenced by the substrate below the implanted region and therefore is not the modulus of amorphous Al_2O_3. This result does show that the modulus of the amorphous material is certainly less than the crystalline sapphire when sampled along the c-axis. This is reasonable since C_{33} is the highest stiffness coefficient for sapphire.

This result leads to difficulties in correcting for elastic recovery of indenter displacement. As previously pointed out, at present the only reasonable way to correct for the elastic effects assumes a constant modulus as function of depth. To properly account for the elastic effects, the elastic recovery of the specimen as a function of depth would have to be determined.

The clearest way to compare the plastic response of the implanted and unimplanted materials is in terms of the ratio of the hardnesses at a given depth. Figures 7(a)(b)(c) show such plots for the three implantations conditions. The comparison in each case is made to the unimplanted data which shows no displacement discontinuities [for instance Fig. 5(b). Since the implanted material shows no such discontinuity, this was judged to be the most reasonable comparison. No corrections for elastic effects have been applied to the data as it is plotted in these curves. Figure 7(c) clearly shows that the amorphous Al_2O_3 is 50% softer than the unimplanted sapphire. This agrees both qualitatively and quantitatively with results from low load (15 g) Knoop indentation results previously reported [7]. The average range of the ions is 80 nm (see Table I) for this specimen and the amorphous phase extends to 155 nm. Hence, the depths at which the softening effects are observed are reasonable.

The result for the specimens implanted with chromium are shown in Figs. 7(a) and (b). There is some very near surface softening shown in Fig. 7(a) that could be due to the residual stress state of the surface. At greater depths a hardening of approximately 4% is observed. This result agrees qualitatively with earlier Knoop indentation test; however, the magnitude of the hardness change is not as large as previously reported. Figure 7(b) shows no significant hardness changes. There are two possible causes for the discrepancy. First, the Knoop indent data may not be quantitatively accurate for reasons already discussed. Second, when apparent hardness is calculated from load displacement curves it is possible for a decreased modulus to compensate for increases in hardness. This is a direct result of the indenter displacement on loading being the sum of the elastic and plastic indentation depths. The reduced modulus detected for the specimen with an amorphous layer indicates that as damage accumulates in the sapphire, the modulus will decrease; hence, a hardness increase could go undetected. Further experiments are planned to determine the modulus as a function of depth for these specimens. Once such data is obtained, the plastic hardness as a function of depth can be properly calculated.

CONCLUSIONS

1. Amorphous Al_2O_3 generated by ion implantation with aluminum and oxygen is 50% softer than single crystal sapphire.

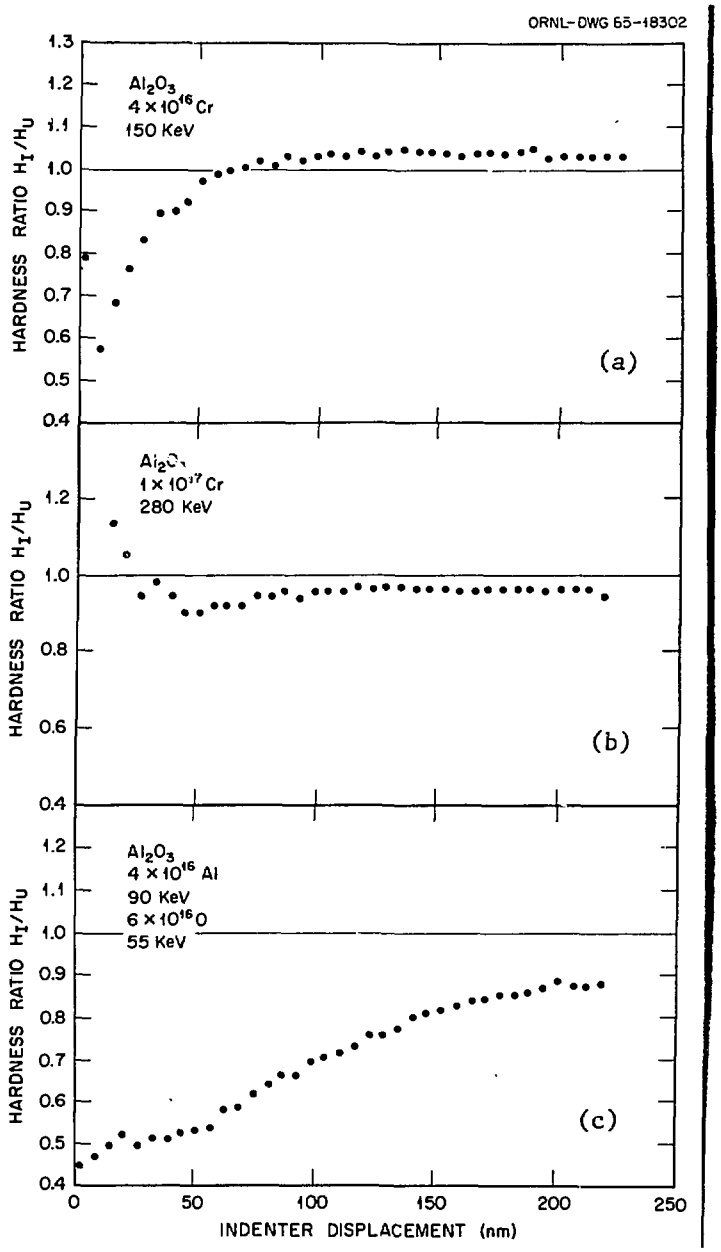

Fig. 7. Comparisons of microindentation results fromimplanted and unimplanted regions of sapphire.

2. No hardness increase has been detected in sapphire implanted with chromium with conditions for which large increases have been previously reported using standard microhardness tests; however, this discrepancy may be due to modulus changes.

3. The stiffness of such amorphous Al_2O_3 is at least 10% lower than the crystalline material as determined with indentation testing.

4. Flaw initiation has been observed at loads of approximately 1 g in well annealed c-axis oriented sapphire.

5. A value of 539 GPa for the modulus of c-axis oriented Al_2O_3 has been determined using indentation testing.

REFERENCES

1. T. Hioki, A. Itoh, S. Noda, H. Doi, J. Kawamoto, and O. Kamigaito, Nucl. Nucl. Instr. Meth. Phys. Res. B, 718, 521–525 (1985).

2. R.W. Rice, P.F. Becher, and W.A. Schmidt, NBS Special Publication No. 348, 1970.

3. C.J. McHargue, International Metals Reviews, in press.

4. C.J. McHargue, G.C. Farlow, C.W. White, B.R. Appleton, J.M. Williams, P.S. Sklad, P. Angelini, and C.S. Yust, in Applications of Ion Plating and Implantation to Materials, edited by R.F. Hochman (ASM, Cleveland, Ohio, in press).

5. C.J. McHargue, C.W. White, B.R. Appleton, G.C. Farlow, and J.M. Williams, in Materials Research Society Symposium Proceedings, Vol. 27 (edited by G.K. Hubler, C.R. Clayton, O.W. Holland, and C.W. White (Elsevier Science Publishers, New York, 1984) pp. 385–394.

6. J.M. Williams, C.J. McHargue, and B.R. Appleton, Nucl. Instr. Meth., 209/210, 317–323 (1983).

7. C.W. White, G.C. Farlow, C.J. McHargue, P.S. Sklad, P. Angelini, and B.R. Appleton, Nucl. Inst. Meth. Phys. Res. B, 7/8, 473–478 (1985).

8. P.J. Burnett and T.F. Page, in Proc. British Ceram. Soc., 34, 65–76 (1984).

9. S.G. Roberts and T.F. Page, in Ion Implantation into Metals, edited by V. Ashworth, W.A. Grant, and R.M. Proctor (Pergamon Press, Elmsford, New York, 1982) pp. 135–146.

10. C.S. Yust, and C.J. McHargue, in Emergent Process Methods for High-Technology Ceramics, Vol. 17, edited by R.F. Davis, H. Palmour III, and R.L. Porter (Plenum Publishing Co., New York, 1984) pp. 533–547.

11. W.C. Oliver, R. Hutchings, and J.B. Pethica, Met. Trans. A., 15A, 2221–2229 (1984).

12. N.A. Stilwell and D. Tabor, Proc. Phys. Soc. London, 78, 169–179 (1961).

13. M.Kh. Shorshorov, S.I. Bulychev, and V.P. Alekhin, Sov. Phys. Doki. 26, No. 8, 769–770 (1981).

14. W.G. Mayer and E.A. Hiedemann, J. Acoust. Soc. Am., 32, 1699–1700 (1960).

15. W.C. Oliver, R. Hutchings, and J.B. Pethica, in Proc. Microindentation Hardness Testing Symposium, July 15–16, 1984, to be published as an ASTM Special Publication.

16. J.L. Loubet, J.M. Georges, O. Marchesini, G. Meille, J. Tribol., 106, 43–48 (1984).

17. R. Hutchings, Mat. Sci. Engr., 69, 129–138 (1985).